# *Measurement of R = B(t→Wb)/B(t→Wq) in top-quark-pair decays using lepton+jets events and the full CDF run II dataset*



**Citation:** Aaltonen, T., S. Amerio, D. Amidei, A. Anastassov, A. Annovi, J. Antos, G. Apollinari, et al. "Measurement of R=B(t→Wb)/B(t→Wq) in top-quark-pair decays using lepton+jets events and the full CDF run II dataset." Physical Review D 87, no. 11 (June 2013). © 2013 American Physical Society

**As Published:** http://dx.doi.org/10.1103/PhysRevD.87.111101

**Publisher:** American Physical Society

**Persistent URL:** http://hdl.handle.net/1721.1/80756

**Version:** Final published version: final published article, as it appeared in a journal, conference proceedings, or other formally published context

PHYSICAL REVIEW D **87,** 111101(R) (2013)

# Measurement of $R = \mathcal{B}(t \to Wb)/\mathcal{B}(t \to Wq)$ in top-quark-pair decays using lepton + jets events and the full CDF run II dataset

T. Aaltonen,[21] S. Amerio,[40a] D. Amidei,[32] A. Anastassov,[15,x] A. Annovi,[17] J. Antos,[12] G. Apollinari,[15] J. A. Appel,[15] T. Arisawa,[53] A. Artikov,[13] J. Asaadi,[48] W. Ashmanskas,[15] B. Auerbach,[2] A. Aurisano,[48] F. Azfar,[39] W. Badgett,[15] T. Bae,[25] A. Barbaro-Galtieri,[26] V. E. Barnes,[44] B. A. Barnett,[23] P. Barria,[42c,42a] P. Bartos,[12] M. Bauce,[40b,40a] F. Bedeschi,[42a] S. Behari,[15] G. Bellettini,[42b,42a] J. Bellinger,[55] D. Benjamin,[14] A. Beretvas,[15] A. Bhatti,[46] K. R. Bland,[5] B. Blumenfeld,[23] A. Bocci,[14] A. Bodek,[45] D. Bortoletto,[44] J. Boudreau,[43] A. Boveia,[11] L. Brigliadori,[6b,6a] C. Bromberg,[33] E. Brucken,[21] J. Budagov,[13] H. S. Budd,[45] K. Burkett,[15] G. Busetto,[40b,40a] P. Bussey,[19] P. Butti,[42b,42a] A. Buzatu,[19] A. Calamba,[10] S. Camarda,[4] M. Campanelli,[28] F. Canelli,[11,15,ee] B. Carls,[22] D. Carlsmith,[55] R. Carosi,[42a] S. Carrillo,[16,m] B. Casal,[9,k] M. Casarsa,[49a] A. Castro,[6b,6a] P. Catastini,[20] D. Cauz,[49a] V. Cavaliere,[22] M. Cavalli-Sforza,[4] A. Cerri,[26,f] L. Cerrito,[28,s] Y. C. Chen,[1] M. Chertok,[7] G. Chiarelli,[42a] G. Chlachidze,[15] K. Cho,[25] D. Chokheli,[13] M. A. Ciocci,[42c,42a] A. Clark,[18] C. Clarke,[54] M. E. Convery,[15] J. Conway,[7] M. Corbo,[15] M. Cordelli,[17] C. A. Cox,[7] D. J. Cox,[7] M. Cremonesi,[42a] D. Cruz,[48] J. Cuevas,[9,z] R. Culbertson,[15] N. d'Ascenzo,[15,w] M. Datta,[15,gg] P. De Barbaro,[45] L. Demortier,[46] M. Deninno,[6a] M. d'Errico,[40b,40a] F. Devoto,[21] A. Di Canto,[42b,42a] B. Di Ruzza,[15,q] J. R. Dittmann,[5] M. D'Onofrio,[27] S. Donati,[42b,42a] M. Dorigo,[49b,49a] A. Driutti,[49a] K. Ebina,[53] R. Edgar,[32] A. Elagin,[48] R. Erbacher,[7] S. Errede,[22] B. Esham,[22] R. Eusebi,[48] S. Farrington,[39] J. P. Fernández Ramos,[29] R. Field,[16] G. Flanagan,[15,u] R. Forrest,[7] M. Franklin,[20] J. C. Freeman,[15] H. Frisch,[11] Y. Funakoshi,[53] A. F. Garfinkel,[44] P. Garosi,[42c,42a] H. Gerberich,[22] E. Gerchtein,[15] S. Giagu,[47a] V. Giakoumopoulou,[3] K. Gibson,[43] C. M. Ginsburg,[15] N. Giokaris,[3] P. Giromini,[17] G. Giurgiu,[23] V. Glagolev,[13] D. Glenzinski,[15] M. Gold,[35] D. Goldin,[48] A. Golossanov,[15] G. Gomez,[9] G. Gomez-Ceballos,[30] M. Goncharov,[30] O. González López,[29] I. Gorelov,[35] A. T. Goshaw,[14] K. Goulianos,[46] E. Gramellini,[6a] S. Grinstein,[4] C. Grosso-Pilcher,[11] R. C. Group,[52,15] J. Guimaraes da Costa,[20] S. R. Hahn,[15] J. Y. Han,[45] F. Happacher,[17] K. Hara,[50] M. Hare,[51] R. F. Harr,[54] T. Harrington-Taber,[15,n] K. Hatakeyama,[5] C. Hays,[39] J. Heinrich,[41] M. Herndon,[55] A. Hocker,[15] Z. Hong,[48] W. Hopkins,[15,g] S. Hou,[1] R. E. Hughes,[36] U. Husemann,[56] M. Hussein,[33,cc] J. Huston,[33] G. Introzzi,[42e,42a] M. Iori,[47b,47a] A. Ivanov,[7,p] E. James,[15] D. Jang,[10] B. Jayatilaka,[15] E. J. Jeon,[25] S. Jindariani,[15] M. Jones,[44] K. K. Joo,[25] S. Y. Jun,[10] T. R. Junk,[15] M. Kambeitz,[24] T. Kamon,[25,48] P. E. Karchin,[54] A. Kasmi,[5] Y. Kato,[38,o] W. Ketchum,[11,hh] J. Keung,[41] B. Kilminster,[15,ee] D. H. Kim,[25] H. S. Kim,[25] J. E. Kim,[25] M. J. Kim,[17] S. B. Kim,[25] S. H. Kim,[50] Y. J. Kim,[25] Y. K. Kim,[11] N. Kimura,[53] M. Kirby,[15] K. Knoepfel,[15] K. Kondo,[53,a] D. J. Kong,[25] J. Konigsberg,[16] A. V. Kotwal,[14] M. Kreps,[24] J. Kroll,[41] M. Kruse,[14] T. Kuhr,[24] M. Kurata,[50] A. T. Laasanen,[44] S. Lammel,[15] M. Lancaster,[28] K. Lannon,[36,y] G. Latino,[42c,42a] H. S. Lee,[25] J. S. Lee,[25] S. Leo,[42a] S. Leone,[42a] J. D. Lewis,[15] A. Limosani,[14,t] E. Lipeles,[41] A. Lister,[18,b] H. Liu,[52] Q. Liu,[44] T. Liu,[15] S. Lockwitz,[56] A. Loginov,[56] D. Lucchesi,[40b,40a] J. Lueck,[24] P. Lujan,[26] P. Lukens,[15] G. Lungu,[46] J. Lys,[26] R. Lysak,[12,e] R. Madrak,[15] P. Maestro,[42c,42a] S. Malik,[46] G. Manca,[27,c] A. Manousakis-Katsikakis,[3] F. Margaroli,[47a] P. Marino,[42d,42a] M. Martínez,[4] K. Matera,[22] M. E. Mattson,[54] A. Mazzacane,[15] P. Mazzanti,[6a] R. McNulty,[27,j] A. Mehta,[27] P. Mehtala,[21] C. Mesropian,[46] T. Miao,[15] D. Mietlicki,[32] A. Mitra,[1] H. Miyake,[50] S. Moed,[15] N. Moggi,[6a] C. S. Moon,[15,aa] R. Moore,[15,ff] M. J. Morello,[42d,42a] A. Mukherjee,[15] Th. Muller,[24] P. Murat,[15] M. Mussini,[6b,6a] J. Nachtman,[15,n] Y. Nagai,[50] J. Naganoma,[53] I. Nakano,[37] A. Napier,[51] J. Nett,[48] C. Neu,[52] T. Nigmanov,[43] L. Nodulman,[2] S. Y. Noh,[25] O. Norniella,[22] L. Oakes,[39] S. H. Oh,[14] Y. D. Oh,[25] I. Oksuzian,[52] T. Okusawa,[38] R. Orava,[21] L. Ortolan,[4] C. Pagliarone,[49a] E. Palencia,[9,f] P. Palni,[35] V. Papadimitriou,[15] W. Parker,[55] G. Pauletta,[49c,49a] M. Paulini,[10] C. Paus,[30] T. J. Phillips,[14] G. Piacentino,[42a] E. Pianori,[41] J. Pilot,[36] K. Pitts,[22] C. Plager,[8] L. Pondrom,[55] S. Poprocki,[15,g] K. Potamianos,[26] A. Pranko,[26] F. Prokoshin,[13,bb] F. Ptohos,[17,h] G. Punzi,[42b,42a] N. Ranjan,[44] I. Redondo Fernández,[29] P. Renton,[39] M. Rescigno,[47a] F. Rimondi,[6a,a] L. Ristori,[42a,15] A. Robson,[19] T. Rodriguez,[41] S. Rolli,[51,i] M. Ronzani,[42b,42a] R. Roser,[15] J. L. Rosner,[11] F. Ruffini,[42b,42a] A. Ruiz,[9] J. Russ,[10] V. Rusu,[15] W. K. Sakumoto,[45] Y. Sakurai,[53] L. Santi,[49c,49a] K. Sato,[50] V. Saveliev,[15,w] A. Savoy-Navarro,[15,aa] P. Schlabach,[15] E. E. Schmidt,[15] T. Schwarz,[32] L. Scodellaro,[9] F. Scuri,[42a] S. Seidel,[35] Y. Seiya,[38] A. Semenov,[13] F. Sforza,[42b,42a] S. Z. Shalhout,[7] T. Shears,[27] P. F. Shepard,[43] M. Shimojima,[50,v] M. Shochet,[11] I. Shreyber-Tecker,[34] A. Simonenko,[13] P. Sinervo,[31] K. Sliwa,[51] J. R. Smith,[7] F. D. Snider,[15] H. Song,[43] V. Sorin,[4] M. Stancari,[15] R. St. Denis,[19] B. Stelzer,[31] O. Stelzer-Chilton,[31] D. Stentz,[15,x] J. Strologas,[35] Y. Sudo,[50] A. Sukhanov,[15] I. Suslov,[13] K. Takemasa,[50] Y. Takeuchi,[50] J. Tang,[11] M. Tecchio,[32] P. K. Teng,[1] J. Thom,[15,g] E. Thomson,[41] V. Thukral,[48] D. Toback,[48] S. Tokar,[12] K. Tollefson,[33] T. Tomura,[50] D. Tonelli,[15,f] S. Torre,[17] D. Torretta,[15] P. Totaro,[40a] M. Trovato,[42d,42a] F. Ukegawa,[50]

 

S. Uozumi,[25] F. Vázquez,[16,m] G. Velev,[15] C. Vellidis,[15] C. Vernieri,[42d,42a] M. Vidal,[44] R. Vilar,[9] J. Vizán,[9,dd] M. Vogel,[35] G. Volpi,[17] P. Wagner,[41] R. Wallny,[8] S. M. Wang,[1] A. Warburton,[31] D. Waters,[28] W. C. Wester III,[15] D. Whiteson,[41,d] A. B. Wicklund,[2] S. Wilbur,[11] H. H. Williams,[41] J. S. Wilson,[32] P. Wilson,[15] B. L. Winer,[36] P. Wittich,[15,g] S. Wolbers,[15] H. Wolfe,[36] T. Wright,[32] X. Wu,[18] Z. Wu,[5] K. Yamamoto,[38] D. Yamato,[38] T. Yang,[15] U. K. Yang,[11,r] Y. C. Yang,[25] W.-M. Yao,[26] G. P. Yeh,[15] K. Yi,[15,n] J. Yoh,[15] K. Yorita,[53] T. Yoshida,[38,l] G. B. Yu,[14] I. Yu,[25] A. M. Zanetti,[49a] Y. Zeng,[14] C. Zhou,[14] and S. Zucchelli[6b,6a]

(CDF Collaboration)

[1]*Institute of Physics, Academia Sinica, Taipei, Taiwan 11529, Republic of China*
[2]*Argonne National Laboratory, Argonne, Illinois 60439, USA*
[3]*University of Athens, Athens 157 71, Greece*
[4]*Institut de Fisica d'Altes Energies, ICREA, Universitat Autonoma de Barcelona, E-08193, Bellaterra (Barcelona), Spain*
[5]*Baylor University, Waco, Texas 76798, USA*
[6a]*Istituto Nazionale di Fisica Nucleare Bologna, Bologna I-40127, Italy*
[6b]*University of Bologna, Bologna I-40127, Italy*
[7]*University of California, Davis, Davis, California 95616, USA*
[8]*University of California, Los Angeles, Los Angeles, California 90024, USA*
[9]*Instituto de Fisica de Cantabria, CSIC-University of Cantabria, 39005 Santander, Spain*
[10]*Carnegie Mellon University, Pittsburgh, Pennsylvania 15213, USA*
[11]*Enrico Fermi Institute, University of Chicago, Chicago, Illinois 60637, USA*
[12]*Comenius University, 842 48 Bratislava, Slovakia; Institute of Experimental Physics, 040 01 Kosice, Slovakia*
[13]*Joint Institute for Nuclear Research, Dubna RU-141980, Russia*
[14]*Duke University, Durham, North Carolina 27708, USA*
[15]*Fermi National Accelerator Laboratory, Batavia, Illinois 60510, USA*
[16]*University of Florida, Gainesville, Florida 32611, USA*
[17]*Laboratori Nazionali di Frascati, Istituto Nazionale di Fisica Nucleare, Frascati I-00044, Italy*
[18]*University of Geneva, CH-1211 Geneva 4, Switzerland*
[19]*Glasgow University, Glasgow G12 8QQ, United Kingdom*
[20]*Harvard University, Cambridge, Massachusetts 02138, USA*
[21]*Division of High Energy Physics, Department of Physics, University of Helsinki and Helsinki Institute of Physics, Helsinki FIN-00014, Finland*
[22]*University of Illinois, Urbana, Illinois 61801, USA*
[23]*The Johns Hopkins University, Baltimore, Maryland 21218, USA*
[24]*Institut für Experimentelle Kernphysik, Karlsruhe Institute of Technology, Karlsruhe D-76131, Germany*
[25]*Center for High Energy Physics: Kyungpook National University, Daegu 702-701, Korea; Seoul National University, Seoul 151-742, Korea; Sungkyunkwan University, Suwon 440-746, Korea; Korea Institute of Science and Technology Information, Daejeon 305-806, Korea; Chonnam National University, Gwangju 500-757, Korea; Chonbuk National University, Jeonju 561-756, Korea; Ewha Womans University, Seoul, 120-750, Korea*
[26]*Ernest Orlando Lawrence Berkeley National Laboratory, Berkeley, California 94720, USA*
[27]*University of Liverpool, Liverpool L69 7ZE, United Kingdom*
[28]*University College London, London WC1E 6BT, United Kingdom*
[29]*Centro de Investigaciones Energeticas Medioambientales y Tecnologicas, E-28040 Madrid, Spain*
[30]*Massachusetts Institute of Technology, Cambridge, Massachusetts 02139, USA*
[31]*Institute of Particle Physics: McGill University, Montréal, Québec H3A 2T8, Canada; Simon Fraser University, Burnaby, British Columbia V5A 1S6, Canada; University of Toronto, Toronto, Ontario M5S 1A7, Canada; and TRIUMF, Vancouver, British Columbia V6T 2A3, Canada*
[32]*University of Michigan, Ann Arbor, Michigan 48109, USA*
[33]*Michigan State University, East Lansing, Michigan 48824, USA*
[34]*Institution for Theoretical and Experimental Physics, ITEP, Moscow 117259, Russia*
[35]*University of New Mexico, Albuquerque, New Mexico 87131, USA*
[36]*The Ohio State University, Columbus, Ohio 43210, USA*
[37]*Okayama University, Okayama 700-8530, Japan*
[38]*Osaka City University, Osaka 588, Japan*
[39]*University of Oxford, Oxford OX1 3RH, United Kingdom*
[40a]*Istituto Nazionale di Fisica Nucleare, Sezione di Padova-Trento, I-35131 Padova, Italy*
[40b]*University of Padova, Padova I-35131, Italy*
[41]*University of Pennsylvania, Philadelphia, Pennsylvania 19104, USA*

[42a]*Istituto Nazionale di Fisica Nucleare Pisa, Pisa I-56127, Italy*
[42b]*University of Pisa, Pisa I-56127, Italy*
[42c]*University of Siena, Pisa I-56127, Italy*
[42d]*Scuola Normale Superiore, Pisa I-56127, Italy*
[42e]*INFN Pavia and University of Pavia, Pavia I-27100, Italy*
[43]*University of Pittsburgh, Pittsburgh, Pennsylvania 15260, USA*
[44]*Purdue University, West Lafayette, Indiana 47907, USA*
[45]*University of Rochester, Rochester, New York 14627, USA*
[46]*The Rockefeller University, New York, New York 10065, USA*
[47a]*Istituto Nazionale di Fisica Nucleare, Roma I-00185, Italy*
[47b]*Sezione di Roma 1, Sapienza Università di Roma, Roma I-00185, Italy*
[48]*Mitchell Institute for Fundamental Physics and Astronomy, Texas A&M University, College Station, Texas 77843, USA*
[49a]*Istituto Nazionale di Fisica Nucleare Trieste/Udine, Trieste I-34127, Italy*
[49b]*University of Trieste, Trieste I-34127, Italy*
[49c]*University of Udine, Udine I-33100, Italy*
[50]*University of Tsukuba, Tsukuba, Ibaraki 305, Japan*
[51]*Tufts University, Medford, Massachusetts 02155, USA*
[52]*University of Virginia, Charlottesville, Virginia 22906, USA*
[53]*Waseda University, Tokyo 169, Japan*
[54]*Wayne State University, Detroit, Michigan 48201, USA*
[55]*University of Wisconsin, Madison, Wisconsin 53706, USA*
[56]*Yale University, New Haven, Connecticut 06520, USA*
(Received 25 March 2013; published 3 June 2013)

We present a measurement of the ratio of the top-quark branching fractions $R = \mathcal{B}(t \to Wb)/\mathcal{B}(t \to Wq)$, where $q$ represents quarks of type $b$, $s$, or $d$, in the final state with a lepton and hadronic jets. The measurement uses $\sqrt{s} = 1.96$ TeV proton-antiproton collision data from 8.7 fb$^{-1}$ of integrated luminosity collected with the Collider Detector at Fermilab during Run II of the Tevatron.

[a]Deceased.
[b]Visitor from University of British Columbia, Vancouver, BC V6T 1Z1, Canada.
[c]Visitor from Istituto Nazionale di Fisica Nucleare, Sezione di Cagliari, 09042 Monserrato (Cagliari), Italy.
[d]Visitor from University of California Irvine, Irvine, CA 92697, USA.
[e]Visitor from Institute of Physics, Academy of Sciences of the Czech Republic, 182 21, Czech Republic.
[f]Visitor from CERN, CH-1211 Geneva, Switzerland.
[g]Visitor from Cornell University, Ithaca, NY 14853, USA.
[h]Visitor from University of Cyprus, Nicosia CY-1678, Cyprus.
[i]Visitor from Office of Science, U.S. Department of Energy, Washington, DC 20585, USA.
[j]Visitor from University College Dublin, Dublin 4, Ireland.
[k]Visitor from ETH, 8092 Zürich, Switzerland.
[l]Visitor from University of Fukui, Fukui City, Fukui Prefecture, Japan 910-0017.
[m]Visitor from Universidad Iberoamericana, Lomas de Santa Fe, México, C.P. 01219, Distrito Federal.
[n]Visitor from University of Iowa, Iowa City, IA 52242, USA.
[o]Visitor from Kinki University, Higashi-Osaka City, Japan 577-8502.
[p]Visitor from Kansas State University, Manhattan, KS 66506, USA.
[q]Visitor from Brookhaven National Laboratory, Upton, NY 11973, USA.
[r]Visitor from University of Manchester, Manchester M13 9PL, United Kingdom.
[s]Visitor from Queen Mary, University of London, London, E1 4NS, United Kingdom.
[t]Visitor from University of Melbourne, Victoria 3010, Australia.
[u]Visitor from Muons, Inc., Batavia, IL 60510, USA.
[v]Visitor from Nagasaki Institute of Applied Science, Nagasaki 851-0193, Japan.
[w]Visitor from National Research Nuclear University, Moscow 115409, Russia.
[x]Visitor from Northwestern University, Evanston, IL 60208, USA.
[y]Visitor from University of Notre Dame, Notre Dame, IN 46556, USA.
[z]Visitor from Universidad de Oviedo, E-33007 Oviedo, Spain.
[aa]Visitor from CNRS-IN2P3, Paris, F-75205 France.
[bb]Visitor from Universidad Tecnica Federico Santa Maria, 110v Valparaiso, Chile.
[cc]Visitor from Yarmouk University, Irbid 211-63, Jordan.
[dd]Visitor from Universite catholique de Louvain, 1348 Louvain-La-Neuve, Belgium.
[ee]Visitor from University of Zürich, 8006 Zürich, Switzerland.
[ff]Visitor from Massachusetts General Hospital and Harvard Medical School, Boston, MA 02114 USA.
[gg]Visitor from Hampton University, Hampton, VA 23668, USA.
[hh]Visitor from Los Alamos National Laboratory, Los Alamos, NM 87544, USA.

We simultaneously measure $R = 0.94 \pm 0.09$ (stat + syst) and the $t\bar{t}$ production cross section $\sigma_{t\bar{t}} = 7.5 \pm 1.0$ (stat + syst) pb. The magnitude of the Cabibbo-Kobayashi-Maskawa matrix element, $|V_{tb}| = 0.97 \pm 0.05$ (stat + syst) is extracted assuming three generations of quarks, and a lower limit of $|V_{tb}| > 0.89$ at 95% credibility level is set.

DOI: 10.1103/PhysRevD.87.111101 PACS numbers: 12.15.Hh, 13.85.Qk, 14.65.Ha

In the standard model (SM) the top-quark decay rate into a $W$ boson and a down-type quark $q$ ($q = d$, $s$, $b$) is proportional to $|V_{tq}|^2$, the squared magnitude of the element of the Cabibbo-Kobayashi-Maskawa (CKM) matrix [1]. Under the assumption of a $3 \times 3$ unitary CKM matrix and using the existing constraints on $V_{ts}$ and $V_{td}$, the magnitude of the top-bottom quark coupling is $|V_{tb}| = 0.99915^{+0.00002}_{-0.00005}$ [2,3], and the top quark decays almost exclusively to $Wb$ final states. Any significant deviation from the expected value would imply new physics: an extra generation of quarks, non-SM top-quark production, or non-SM background to top-quark production. A direct measurement of the magnitude of the $V_{tb}$ matrix element can be obtained from the single-top-quark production cross section [4], which is proportional to $|V_{tb}|^2$. The value of $|V_{tb}|$ can also be extracted from the decay rate of pair-produced top quarks. We define $R$ as the ratio of the branching fractions

$$R = \frac{\mathcal{B}(t \to Wb)}{\mathcal{B}(t \to Wq)}. \quad (1)$$

Given the unitarity of the CKM matrix and assuming three generations, $R$ is indirectly determined by the knowledge of $V_{ts}$ and $V_{td}$,

$$R = \frac{|V_{tb}|^2}{|V_{tb}|^2 + |V_{ts}|^2 + |V_{td}|^2}, \quad (2)$$

and is derived to be $0.99830^{+0.00004}_{-0.00009}$ [2]. A deviation from this prediction would be an indication of non-SM physics.

This paper reports the first CDF simultaneous measurement of $R$ and top-quark-pair-production cross section $\sigma_{t\bar{t}}$ performed on a data sample corresponding to an integrated luminosity of 8.7 fb$^{-1}$ collected with the CDF II detector [5] at the Fermilab Tevatron $p\bar{p}$ Collider at center of mass energy $\sqrt{s} = 1.96$ TeV. The analysis uses events with a lepton and multiple jets in the final state, where one $W$ boson coming from $t\bar{t}$ production decays into a quark and an antiquark, while the second $W$ boson decays into a charged lepton (electron or muon) and a neutrino.

CDF has performed several measurements of $R$ during both Run I and Run II, combining the lepton + jets final state with the dilepton final state, where both $W$ bosons decay into leptons. The most recent publication reported $R = 1.12^{+0.21}_{-0.19}(\text{stat})^{+0.17}_{-0.13}(\text{syst})$ and $R > 0.61$ at 95% confidence level (C.L.) using 162 pb$^{-1}$ of integrated luminosity [6]. The D0 Collaboration measured $R = 0.90 \pm 0.04$ (stat + syst) and $R > 0.79$ at 95% C.L. [7], using data from 5.4 fb$^{-1}$ of integrated luminosity, in the lepton + jets and dilepton final states combined.

The CDF II detector [5] consists of a charged-particle tracking system in a magnetic field of 1.4 T, segmented electromagnetic and hadronic calorimeters with a pointing geometry, and muon detectors. A silicon microstrip detector provides determination of charged-particle trajectories (tracking) over the radial range 1.5 to 28 cm, and is essential for the detection of displaced decay (secondary) vertices. A three-level, online event-selection system (trigger) [8] is used to select events with an electron (muon) candidate in the central detector region (pseudorapidity $|\eta| < 1.1$) [9], with $E_T$ ($p_T$) $> 18$ GeV (18 GeV/$c$), which form the data set for this analysis.

The measurement of $R$ is based on the determination of the number of $b$-quark jets in $t\bar{t}$ events reconstructed in the lepton + jets final state. The lepton + jets signature consists of a high-$p_T$ charged electron ($e$) or muon ($\mu$), large missing transverse energy $\not\!\!E_T$ [9] due to the undetected neutrino from the leptonic $W$ decay, and at least three hadronic jets. Events containing muons are classified according to the coverage of the detectors used for their identification as central, when $|\eta| < 0.6$, and forward, when $0.6 < |\eta| < 1.0$. Identification of jets coming from $b$-quark fragmentation ($b$-jet tagging) is performed by the SECVTX algorithm, which is based on the reconstruction of secondary vertices displaced from the primary $p\bar{p}$ interaction vertex and selects a sample enriched with jets originating from $b$ quarks [10]. The lepton + jets selection requirements are described in Ref. [10]. Briefly, the analysis requires the presence of one isolated lepton ($e$ or $\mu$) with $E_T$ greater than 20 GeV, $\not\!\!E_T$ of at least 20 GeV, and a minimum of three jets, reconstructed using a cone algorithm [11] with radius $\Delta R = 0.4$ in $\eta - \phi$ space [9], within $|\eta| < 2.0$. The jet $E_T$, after correcting for the calorimeter response [11], has to exceed 30, 25, and 20 GeV for the most energetic, second-most-energetic, and any additional jet in the event, respectively. The $W$-boson transverse mass [9] is required to be greater than 20 GeV/$c^2$. Events with one or two identified $b$ jets are selected (1 $b$-tag and 2 $b$-tag events, respectively).

The background processes include $W$-boson production in association with heavy-flavor jets ($Wb\bar{b}$, $Wc\bar{c}$, $Wc$), or in association with light-flavor jets that are incorrectly identified as $b$ jets ("mistags"), quantum chromodynamics multijet ("QCD") events containing misreconstructed or real leptons or incorrectly measured $\not\!\!E_T$, diboson events ($WW$, $WZ$, $ZZ$), single-top-quark production, and $Z$ + jets events.

We divide the selected sample into subsets according to the type of lepton, number of jets in the final state, and number of identified $b$ jets (one or two). As explained in more detail below, we derive an expected event yield for each category. We then maximize the likelihood for observing the events found in each category by varying two fit parameters, $R$ and the top-quark-pair-production cross section $\sigma_{t\bar{t}}$.

The $t\bar{t}$ events are modeled using the PYTHIA [12] Monte Carlo (MC) generator with top-quark mass $m_t = 172.5\ \mathrm{GeV}/c^2$. We estimate the backgrounds with a collection of data-driven and simulation techniques described in Ref. [10]. The QCD background is modeled using data control samples [13]. Mistags are estimated using a matrix (the mistag matrix) calculated in control samples and parametrized as a function of jet and event characteristics [13]. Diboson processes are simulated using PYTHIA; single-top-quark production is simulated by POWHEG [14], while the parton shower and fragmentation is provided by PYTHIA. The ALPGEN [15] generator, with PYTHIA supplying the parton shower and fragmentation, is used to model the $W$ + jets and $Z$ + jets backgrounds. A GEANT-based simulation is used to model the response of the CDF II detector [16]. The cross sections used for background normalization can be found in Ref. [13]. Table I shows the expected sample composition for all final states, after summing over lepton categories, assuming $R = 1$ and $\sigma_{t\bar{t}} = 7.04 \pm 0.49$ pb [17].

The number of $b$-tagged events is the most sensitive quantity to possible values of $R$ different from one: the smaller $R$, the smaller the probability to have a $b$ jet in a top-quark-pair event. Hence, the fraction of events with one or two tags is expected to decrease with decreasing $R$. In general, the $t\bar{t}$ production cross section measured by CDF in the lepton + jets sample assumes $R = 1$. In order to avoid any bias due to this premise, we measure simultaneously $R$ and the production cross section, since the measurement of the latter is affected by the sum of events in the different tag bins.

To perform the fit, we first divide the sample into 18 independent subsamples, organized by type of lepton, number of jets in the event (3, 4, $\geq$5), and number of identified $b$ jets. The expected number of events in each subsample, $\mu^{i,j}_{\mathrm{exp}}$, is given by the following expression:

$$\mu^{i,j}_{\mathrm{exp}} = \mu^{i,j}_{t\bar{t}} + N^{i,j}_B = \mathcal{L}^j \epsilon^{i,j}_{\mathrm{evt}} \sigma_{t\bar{t}} \epsilon^i_{\mathrm{tag}}(R) + N^{i,j}_B, \quad (3)$$

where $\mu^{i,j}_{t\bar{t}}$ is the expected number of $t\bar{t}$ events and $N^{i,j}_B$ the expected number of background events. The $i$ and $j$ indices indicate the $i$th jet bin with one or two identified $b$ jets (jet-tag category) and the $j$th lepton category, respectively. $\mathcal{L}^j$ is the integrated luminosity, $\epsilon^{i,j}_{\mathrm{evt}}$ includes the trigger and lepton identification efficiencies, and $\epsilon^i_{\mathrm{tag}}(R)$ is the event-tagging efficiency, i.e., the efficiency for tagging at least one jet in an event. In an ideal case without background and assuming a $b$-tagging efficiency equal one for jets originating from $b$ quarks and zero for jets originating from non-$b$ quarks, the number of expected events with two tags is proportional to $R^2$, while the number of expected events with one tag is proportional to $2R(1 - R)$. The estimates for the background processes are calculated with various values of $R$. The differences with respect to the estimates obtained with $R = 1$ are found to be negligible.

The event-tagging efficiencies are calculated in $t\bar{t}$ MC samples, using the probability to tag a jet as a $b$ jet according to the SECVTX algorithm, on a jet-by-jet basis. For jets originated from $b$ and $c$ quarks, the $b$-jet tagging efficiencies are corrected for differences between data and MC using a scale factor $\mathrm{SF} = 0.96 \pm 0.05$ [18]. For jets originated from light-flavor quarks, the probability to tag them as $b$ jets is obtained using the mistag matrix.

In general, $\epsilon^i_{\mathrm{tag}}$ is calculated from the event probability to tag the $m$th event in MC processes with possible $b$-quark final states. For an event with $n$ generic jets, the probability to have one [Eq. (4)] or two [Eq. (5)] tagged $b$ jets becomes

TABLE I. Number of expected and observed events in lepton + jets data corresponding to 8.7 fb$^{-1}$ of integrated luminosity. Uncertainties include statistical and systematic contributions.

| | 1 $b$-tag | | | 2 $b$-tag | | |
|---|---|---|---|---|---|---|
| Process | 3 Jets | 4 Jets | $\geq$5 Jets | 3 Jets | 4 Jets | $\geq$5 Jets |
| $t\bar{t}$ | $800 \pm 67$ | $777 \pm 64$ | $260 \pm 21$ | $216 \pm 30$ | $271 \pm 36$ | $97 \pm 13$ |
| $W + b\bar{b}$ | $291 \pm 118$ | $74 \pm 30$ | $17 \pm 7$ | $48 \pm 20$ | $14 \pm 6$ | $4 \pm 2$ |
| $W + c\bar{c}$ | $167 \pm 68$ | $47 \pm 20$ | $12 \pm 5$ | $5 \pm 2$ | $2 \pm 1$ | $0.8 \pm 0.4$ |
| $W + c$ | $87 \pm 35$ | $17 \pm 7$ | $4 \pm 2$ | $3 \pm 1$ | $0.8 \pm 0.4$ | $0.2 \pm 0.1$ |
| Single top | $78 \pm 7$ | $17 \pm 2$ | $3.6 \pm 0.3$ | $18 \pm 3$ | $4.7 \pm 0.7$ | $1.1 \pm 0.2$ |
| Diboson | $45 \pm 5$ | $11 \pm 1$ | $3.1 \pm 0.3$ | $3.1 \pm 0.5$ | $0.9 \pm 0.1$ | $0.30 \pm 0.05$ |
| $Z$ + jets | $32 \pm 3$ | $9.1 \pm 0.9$ | $2.4 \pm 0.2$ | $2.1 \pm 0.2$ | $0.77 \pm 0.08$ | $0.29 \pm 0.03$ |
| Mistags | $303 \pm 42$ | $74 \pm 14$ | $17 \pm 6$ | $5 \pm 1$ | $1.7 \pm 0.4$ | $0.6 \pm 0.2$ |
| QCD | $125 \pm 50$ | $35 \pm 29$ | $10 \pm 9$ | $6 \pm 3$ | $0.1 \pm 1.5$ | $0.1 \pm 1.5$ |
| Total prediction | $1928 \pm 243$ | $1061 \pm 93$ | $330 \pm 28$ | $306 \pm 40$ | $296 \pm 38$ | $104 \pm 13$ |
| Observed | 1844 | 1088 | 339 | 275 | 273 | 126 |

$$P^m_{1-\mathrm{tag}} = \sum_{q=1}^{n} p_q^{\mathrm{tag}} \Big( \prod_{r=1, r\neq q}^{n} (1 - p_r^{tag}) \Big) \quad (4)$$

$$P^m_{2-\mathrm{tag}} = \sum_{q=1}^{n-1} p_q^{\mathrm{tag}} \Big( \sum_{r>q}^{n} p_r^{\mathrm{tag}} \Big( \prod_{s=1, s\neq q, s\neq r}^{n} (1 - p_s^{\mathrm{tag}}) \Big) \Big), \quad (5)$$

where $p_q^{\mathrm{tag}}$ is either the probability to tag the $q$th jet, multiplied by the SF, for jets where the heavy-flavor quark is found inside the jet cone, or the mistag probability for jets matched to a light-flavor hadron, calculated using the mistag matrix.

Finally, we use the $P^m_{l-\mathrm{tag}}$ as an event weight to calculate the event-tagging efficiency $\epsilon^i_{\mathrm{tag}}$ for each subsample with $l$ tags and $n$ jets by summing the $P^m_{l-\mathrm{tag}}$ weights over all of the pretagged events.

The MC sample employed for the $t\bar{t}$ signal modeling is generated assuming $|V_{\mathrm{tb}}| = 1$, so it cannot be used directly to calculate $\epsilon^i_{\mathrm{tag}}$ as a function of $R$ through the algorithm described above. Instead, in the MC sample we assign a uniform random number $P_b$ in the interval [0, 1] to every jet that is matched at the parton level to a $b$ quark from $t$-quark decay. If $P_b < R$ we consider this jet as genuinely originated by a $b$ quark and use the tag probability multiplied by the SF as in Eqs. (4) and (5); otherwise, this jet is regarded as a light-flavor jet. This simulates a configuration in which a $b$ quark produced in the top decay is a real $b$ only $R$ fraction of the time, while $(1 - R)$ fraction of the time it is treated as a light-flavor quark and it is weighted by the mistag probability. This probabilistic approach allows the calculation of background and signal sample composition for any value of $R$. This method reproduces exactly the standard calculation in the case of $R = 1$, simulates $t \to Wq$ for $R = 0$, and allows a calculation of $\epsilon^i_{\mathrm{tag}}(R)$ in each tag subsample and in each jet bin. Figure 1 shows the comparison of observed and expected events assuming $R$ equal to 1, 0.5, and 0.1 in the various jet multiplicities and number of $b$-tagged jets in the final state.

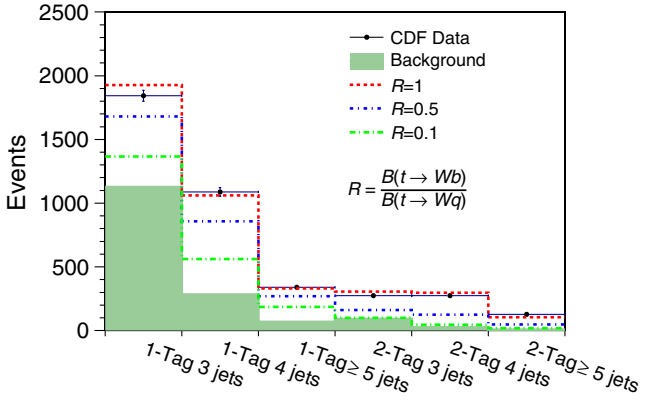


FIG. 1 (color online). Observed events for the analysis final states after summing over lepton categories, compared to expected events for different values of $R$. For the $t\bar{t}$ normalization the theoretical value $\sigma_{t\bar{t}} = 7.04 \pm 0.49$ pb is used.

In order to compare the prediction to the observed data in the 18 subsamples, we use a likelihood function. We fit the observed event yields in each class of events to determine simultaneously $R$ and $\sigma_{t\bar{t}}$. The likelihood function is

$$\mathcal{L} = \prod_{i,j} \mathcal{P}(\mu^{i,j}_{\mathrm{exp}}(R, \sigma_{t\bar{t}}, x_a) | N^{i,j}_{\mathrm{obs}}) \prod_a G(x_a | 0, 1), \quad (6)$$

where $\mathcal{P}(\mu^{i,j}_{\mathrm{exp}}(R, \sigma_{t\bar{t}}, x_a) | N^{i,j}_{\mathrm{obs}})$ is the Poisson probability to observe $N^{i,j}_{\mathrm{obs}}$ events assuming the expected mean $\mu^{i,j}_{\mathrm{exp}}$ [given by Eq. (3)], the index $i$ indicates the jet-tag category, and the index $j$ runs over the different lepton categories. The estimates of the nuisance parameters $x_a$ are constrained to their central values and normalized to their uncertainties using Gaussian distributions $G(x_a|0, 1)$ centered at zero with unit variance. This procedure takes into account correlations among channels by using same parameters for common sources of systematic uncertainties and allowing variations of each parameter with respect to its central value.

We perform the minimization of the negative logarithm of the likelihood $-2\log(\mathcal{L})$, using the MINUIT package [19]. We analytically extend $\epsilon^i_{\mathrm{tag}}(R)$ beyond $R = 1$ during the fitting procedure, constraining each individual $\epsilon^i_{\mathrm{tag}}(R)$ to be greater than zero and their sum to be $\leq 1$. We simultaneously fit $R$ and $\sigma_{t\bar{t}}$, which are the free parameters of the likelihood. We update the calculation of background yields using the value of $\sigma_{t\bar{t}}$ determined by the fit and iterate the previous steps until the procedure converges. No dependence on the starting point was observed in the results of the iterative procedure.

The uncertainty determined by the fit comprises the statistical contribution; the systematic contribution on event-tagging efficiency; the event selection efficiency; the background normalizations; corrections for differences between MC and data heavy-flavor yields; and the luminosity [13]. We include separately the contributions due to the uncertainty on the jet-energy scale, effect of initial- and final-state radiation in the simulation (ISR/FSR), event-generator dependences, and top-quark mass. The impact of the jet-energy scale uncertainty is estimated by varying the energy of all jets in the MC samples by $\pm 1$ standard deviation with respect to the central value for both signal and backgrounds and by repeating the iterative fits. The uncertainty arising from the choice of the MC generator is evaluated by repeating the analysis using a $t\bar{t}$ sample generated by HERWIG [20]. The ISR/FSR uncertainty is evaluated by using $t\bar{t}$ MC samples generated with enhanced or suppressed radiation relative to the default configuration. The theoretical value of the top-quark-production cross section depends on top-quark mass [21]. The recursive fit of $\sigma_{t\bar{t}}$ is expected to reduce the impact of this systematic uncertainty. In order

TABLE II. Systematic uncertainties on the measurement of $R$ and $\sigma_{t\bar{t}}$ obtained from simulated experiments. "Others" indicates the squared sum of minor systematic uncertainties. All systematic uncertainties are assumed to be fully uncorrelated. The statistical uncertainty is shown as well.

| Source | $+\delta R$ | $-\delta R$ | $+\delta\sigma_{t\bar{t}}$ (pb) | $-\delta\sigma_{t\bar{t}}$ (pb) |
|---|---|---|---|---|
| $b$-tagging | 0.078 | −0.073 | 0.06 | −0.03 |
| Background normalization | 0.056 | −0.052 | 0.78 | −0.66 |
| Jet-energy scale | 0.016 | −0.019 | 0.46 | −0.41 |
| ISR/FSR | 0.006 | −0.006 | 0.22 | −0.21 |
| Luminosity | 0.001 | −0.002 | 0.44 | −0.39 |
| Top-quark mass | 0.001 | −0.000 | 0.33 | −0.32 |
| Others | 0.005 | −0.006 | 0.17 | −0.15 |
| Total syst. uncert. | 0.088 | −0.081 | 1.04 | −0.92 |
| Statistical | 0.043 | −0.043 | 0.29 | −0.29 |

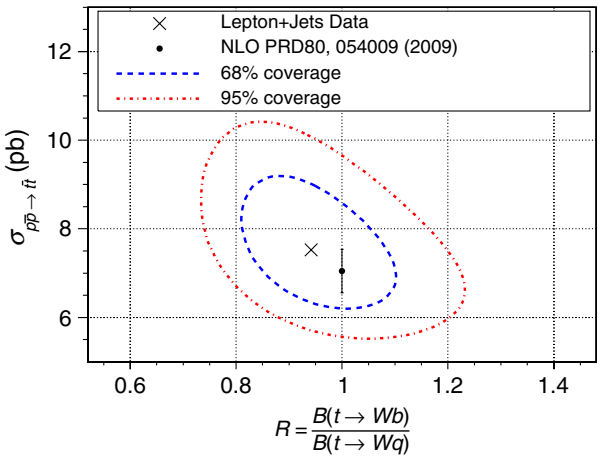


FIG. 2 (color online). The fit results for the simultaneous measurement of $R$ and $\sigma_{t\bar{t}}$. The X-cross corresponds to the maximum of the likelihood; the point with error bar to the NLO cross section calculation. The two-dimensional confidence regions are shown as well.

to check this assumption, we repeat the measurement using two different MC samples for the $t\bar{t}$ signal, simulated with $m_t = 170\ \mathrm{GeV}/c^2$ and $m_t = 175\ \mathrm{GeV}/c^2$, respectively. Central values and uncertainties on those systematic effects are included in the likelihood as nuisance parameters.

As a consistency check, the effect of each source of systematic uncertainty is estimated via simulated experiments. For each source we generate a set of simulated experiments with the same prescription but with the nuisance parameter $x_a$, relative to the systematic effect under study, shifted by one standard deviation from its nominal value. We determine the effect of changing each source of systematic uncertainty as the change in the mean of the distributions of $R$ and $\sigma_{t\bar{t}}$. Table II lists the various systematic uncertainties assumed as fully uncorrelated.

We measure $R = 0.94 \pm 0.09$ and $\sigma_{t\bar{t}} = 7.5 \pm 1.0$ pb with a correlation $\rho = -0.434$. Figure 2 shows the two-dimensional likelihood contour in the $(R, \sigma_{t\bar{t}})$ plane, for the fit including statistical and systematic uncertainties. The results are in agreement with the theoretical prediction [17] to within one standard deviation.

To determine the credibility level limit on $R$, we follow a Bayesian statistical approach. Since $R$ is bounded to be in the interval [0,1], the prior probability density is chosen to be zero outside these $R$ boundaries, while we consider all physical values equally probable. To obtain the posterior distribution for $R$, we integrate over all nuisance parameters using non-negative normal distributions as priors. We also integrate over $\sigma_{t\bar{t}}$ with the only constraint to be positive defined.

The Bayesian lower limits are $R > 0.785$ (0.876) at 95 (68) % credibility level (CL) [22]. From Eq. (1) we extract a measurement of $V_{\mathrm{tb}}$. Assuming three generations of quarks and given the unitarity of the CKM matrix, we get $R = |V_{\mathrm{tb}}|^2$. From the fit results we obtain $|V_{\mathrm{tb}}| = 0.97 \pm 0.05$ and $|V_{\mathrm{tb}}| > 0.89$ at 95% C.L.

In summary, we present the simultaneous measurement of $R = 0.94 \pm 0.09$ and $\sigma_{t\bar{t}} = 7.5 \pm 1.0$ pb, and the determination of $|V_{\mathrm{tb}}| = 0.97 \pm 0.05$. The results for $R$ and $|V_{\mathrm{tb}}|$ are the most precise determination obtained by CDF and are in agreement with the standard model [2], with the previous CDF measurements [6], with the latest measurement of $R$ performed by D0 [7], and with the direct measurement of single-top-quark production cross section performed by LHC [23] and Tevatron [4,24] experiments.

We thank the Fermilab staff and the technical staffs of the participating institutions for their vital contributions. This work was supported by the U.S. Department of Energy and National Science Foundation; the Italian Istituto Nazionale di Fisica Nucleare; the Ministry of Education, Culture, Sports, Science and Technology of Japan; the Natural Sciences and Engineering Research Council of Canada; the National Science Council of the Republic of China; the Swiss National Science Foundation; the A. P. Sloan Foundation; the Bundesministerium für Bildung und Forschung, Germany; the Korean World Class University Program, the National Research Foundation of Korea; the Science and Technology Facilities Council and the Royal Society, UK; the Russian Foundation for Basic Research; the Ministerio de Ciencia e Innovación, and Programa Consolider-Ingenio 2010, Spain; the Slovak R&D Agency; the Academy of Finland; and the Australian Research Council (ARC).

[1] N. Cabibbo, Phys. Rev. Lett. **10**, 531 (1963); M. Kobayashi and T. Maskawa, Prog. Theor. Phys. **49**, 652 (1973).

[2] J. Beringer *et al.* (Particle Data Group), Phys. Rev. D **86**, 010001 (2012).

[3] A. Abulencia *et al.* (CDF Collaboration), Phys. Rev. Lett. **97**, 242003 (2006); V. M. Abazov *et al.* (D0 Collaboration), Phys. Rev. Lett. **97**, 021802 (2006); R. Aaij *et al.* (LHCb Collaboration) Phys. Lett. B **709**, 177 (2012).

[4] V. M. Abazov *et al.* (D0 Collaboration), Phys. Rev. Lett. **103**, 092001 (2009); T. Aaltonen *et al.* (CDF Collaboration), Phys. Rev. Lett. **103**, 092002 (2009).

[5] D. Acosta *et al.* (CDF Collaboration), Phys. Rev. D **71**, 032001 (2005).

[6] D. Acosta *et al.* (CDF Collaboration) Phys. Rev. Lett. **95**, 102002 (2005).

[7] V. M. Abazov *et al.* (D0 Collaboration) Phys. Rev. Lett. **107**, 121802 (2011).

[8] R. Downing, N. Eddy, L. Holloway, M. Kasten, H. Kim, J. Kraus, C. Marino, K. Pitts, J. Strologas, and A. Taffard, Nucl. Instrum. Methods Phys. Res., Sect. A **570**, 36 (2007).

[9] We use a cylindrical coordinate system where the $z$ axis is along the proton beam direction, $\phi$ is the azimuthal angle, and $\theta$ is the polar angle. Pseudorapidity is $\eta = -\ln\tan(\theta/2)$, while transverse momentum is $p_T = |p|\sin\theta$, and transverse energy is $E_T = E\sin\theta$. Missing transverse energy, $\not\!\!E_T$, is defined as the magnitude of $-\sum_i E_T^i \hat{n}_i$, where $\hat{n}_i$ is the unit vector in the azimuthal plane that points from the beam line to the $i$th calorimeter tower. The $W$ boson transverse mass is defined as $M_T^W = \frac{1}{c^2}\sqrt{2E_T^l \not\!\!E_T(1-\cos\phi_{l\nu})}$, where $E_T^l$ is the transverse energy of the lepton and $\phi_{l\nu}$ is the angle between the lepton and the $\not\!\!E_T$.

[10] D. Acosta *et al.* (CDF Collaboration), Phys. Rev. D **71**, 052003 (2005).

[11] A. Bhatti *et al.*, Nucl. Instrum. Methods Phys. Res., Sect. A **566**, 375 (2006).

[12] T. Sjostrand, P. Eden, C. Friberg, L. Lonnblad, G. Miu, S. Mrenna, and E. Norrbin, Comput. Phys. Commun. **135**, 238 (2001).

[13] T. Aaltonen *et al.* (CDF Collaboration), Phys. Rev. D **86**, 032011 (2012).

[14] S. Alioli, P. Nason, C. Oleari, and E. Re, J. High Energy Phys. 09 (2009) 111.

[15] M. L. Mangano, F. Piccinini, and A. Polosa, J. High Energy Phys. 07 (2003) 001.

[16] S. Agostinelli *et al.*, Nucl. Instrum. Methods Phys. Res., Sect. A **506**, 250 (2003).

[17] U. Langenfeld, S. Moch, and P. Uwer, Phys. Rev. D **80**, 054009 (2009).

[18] T. Aaltonen *et al.* (CDF Collaboration), Phys. Rev. D **85**, 072001 (2012).

[19] F. James, MINUIT Reference Manual, Version 94.1, CERN Program Library Long Write-up D506 (1994).

[20] G. Corcella, I. G. Knowles, G. Marchesini, S. Moretti, K. Odagiri, P. Richardson, M. H. Seymour, and B. R. Webber, J. High Energy Phys. 01 (2001) 010.

[21] M. Cacciari, S. Frixione, M. L. Mangano, P. Nason, and G. Ridolfi, J. High Energy Phys. 09 (2008) 127; N. Kidonakis and R. Vogt, Phys. Rev. D **78**, 074005 (2008).

[22] See Supplemental Material at http://link.aps.org/supplemental/10.1103/PhysRevD.87.111101 for posterior probability density showing the 68% and 95% CL limits for R.

[23] G. Aad *et al.* (ATLAS Collaboration), Phys. Lett. B **717**, 330 (2012); S. Chatrchyan *et al.* (CMS Collaboration), J. High Energy Phys. 12 (2012) 035; Phys. Rev. Lett. **110**, 022003 (2013).

[24] V. M. Abazov *et al.* (D0 Collaboration), Phys. Lett. B **703**, 422 (2011).